DEVELOPMENT AND ENGINEERING APPLICATION OF STRONG PERMEABILITY GROUTING MATERIAL FOR WEATHERED GRANITE FORMATION

CHUNQUAN DAI* , YANXIA LONG, ZEJUN SHI, GUANGXUE XING, WENZENG HOU
Key Laboratory of Disaster Prevention and Reduction of Civil Engineering in Shandong Province, Qingdao 266590, China
College of Civil Engineering and Architecture, Shandong University of Science and Technology, Qingdao 266590, China

Considering the high permeability and low strength of weathered granite in tunnelling and underground projects, this paper develops strong permeability grouting (SPG) materials with good fluidity, excellent impermeability and long durability based on the features of the weathered granite formation. The materials can repair and reinforce the weathered granite formation through permeation grouting. Besides, the author tested the basic mechanical properties of the proposed SPG materials, and applied them to a tunnelling project of Qingdao Metro. The test and application results show that the SPG materials enjoy great wettability and permeability to granite; the SPG materials can meet the requirements for grouting projects in granite formation, due to the good strength and impermeability of their concretions; the SPG slurries require easy steps and a low grouting pressure in construction. The promotion and application of the proposed SPG materials will definitely bring good economic and social benefits, owing to the huge demand for high-performance grouting materials at home and abroad.

Keywords: *Grouting Material; Weathered Granite; Orthogonal Test; Permeability*

1. Introduction

In underground engineering, the construction team often encounters deep, thick formation of intensely, if not completely, weathered granite with a high water content. Such a formation is weak, unstable and very sensitive to water seepage. It is prone to such geological disasters as collapse and water or mud inrush [1,2]. To prevent these disasters, tunnel construction mainly relies on grouting to realize water plugging and reinforcement [3-9]. So far, many effective grouting methods have been developed to solve the geological problems of complex weathered granite formation, including splitting-permeation grouting [10], clay grouting [11], segment grouting with horizontally-retracting drill rod [12], composite grouting, reinforcement and excavation [13], full-section curtain grouting [14] and curtain grouting dynamic treatment [15].

The grouting material is a key determinant of the grouting effect, alongside with many other influencing factors. The correct and rational selection of the grouting material directly bears on the success and economic benefit of the grouting project. In undergrounding engineering, the existing grouting materials mainly include cement slurry [16], water glass slurry, water glass-cement slurry [17], organic polymer chemical grouting material and composite slurry [18]. However, these traditional grouting materials can only enhance the grouting pressure, failing to achieve permeation grouting.

Even if they are implemented in a composite manner, the grouting effect is still undesirable despite the complicated operations. This calls for a new high-performance grouting material that overcomes the defects of traditional materials in dealing with the engineering problems caused by weathered granite. Such a material will definitely promote the development of grouting technology and the construction of underground projects.

Considering the high permeability and low strength of weathered granite in tunnelling and underground projects, this paper develops strong permeability grouting (SPG) materials with good fluidity, excellent impermeability and long durability based on the features of the weathered granite formation. The materials can repair and reinforce the weathered granite formation through permeation grouting. Besides, the author examined the mechanical properties and the engineering application effect of the proposed SPG materials, laying the basis for further promotion of the material.

2. Basic Performance Test on SPG Material

2.1. Test materials

(1) Metakaolin

The metakaolin for preparing grouting material was produced through high-temperature calcination of the kaolin powder purchased from a kaolin company in Gongyi, central China's Henan Province.

(2) Silica sol

Silica sol, a special nano-material, is a colloidal solution formed by uniformly dispersing amorphous SiO_2 aggregates in water. The material is odourless, non-toxic and non-corrosive. In our test, the silica sol is the JN-30 type produced by Qingdao Haiyang Chemical Co., Ltd. The performance indices of the silica sol are listed in Table 1.

* Autor corespondent/*Corresponding author*,
E-mail: dcqwin@sdust.edu.cn

Table 1

Performance indices of the silica sol

SiO_2 content (%)	Na_2O content ≤ (%)	pH	Viscosity 25℃ (mpa·s)	Density 25℃ (g/cm^3)	Mean particle size (nm)
30.0-31.0	0.30	8.5-10.0	7.0	1.19-1.21	10-20

Table 2

Factors and levels of the orthogonal test

Level	Factor				
	A (silica sol dosage)	B (silicon powder dosage)	C (Quicklime dosage)	D (RLP dosage)	E (composite additive dosage)
1	30	10	5	1	1
2	40	15	10	3	4
3	50	20	15	5	7
4	60	25	20	7	10

(3) Silicon powder

Silicon powder is an ultrafine powder formed through the oxidation between the air and highly volatile SiO_2 and silicon vapour, which are produced in the ore-smelting electric furnace during the smelting of silicon iron and industrial silicon. The silicon powder for our test, purchased from Guizhou Zunyi Ferrosilicon Alloy Factory, consists of 90.75% SiO_2, 3.62% Fe_2O_3, 1.87 Al_2O_3, 0.35% CaO, 1.32% MgO and 0.27% SO_3.

(4) Quicklime

The quicklime was purchased from the market, which contains CaO, MgO, CO_2 and SO_3.

(5) Redispersible latex powder (RLP)

The RLP is a polymer powder obtained by spray drying of synthetic resin emulsion, added with a modifier. The powder can form an emulsion after being mixed with water. The RLP for our test was purchased from Wacker Chemie AG. The main content is a copolymer of vinyl acetate and ethylene.

(6) Composite additive

The composite additive was a light yellow powder self-made from four kinds of surfactants.

(7) Water

Tap water was used for lab tests. On the construction site, the tester can use nearby tap water, clean groundwater and river water.

2.2. Test method

The performance of grouting material can be measured by many indices. Among them, the key, basic indices that affect the grouting effect are the initial viscosity of the slurry, the gelation time, the sweating rate, the permeability coefficient of the concretion, and the 28d compressive strength. To reduce the workload, only these key indices of the grouting material were measured in the orthogonal test that determines the initial mix proportion. The test design is detailed as follows. Taking the metakaolin amount (fixed amount) as the benchmark, the basic properties of slurry and concretion were tested after adding different proportions of silica sol, silicon powder, quicklime, RLP and composite additive, aiming to determine the initial mix proportion of the grouting material for each purpose. The mix proportions of all components in the orthogonal test were designed after a thorough literature review and repeated preparatory tests. The test covers 5 factors and 4 levels according to the L16(45) orthogonal test chart (Table 2).

The main performance of the grouting material was tested by the orthogonal test in the following steps.

(1) Initial viscosity of the slurry

In engineering practice, the slurry viscosity usually means the relative viscosity, i.e. the viscosity ratio of a fluid to water at the same temperature. In our test, the slurry viscosity was measured by a 1006 type funnel viscometer, which counts the time needed for 500mL slurry to flow out of the viscometer (unit: s).

(2) Gelation time

The gelation time of the slurry was measured by an NDJ-1 type rotary viscometer. The time history of slurry viscosity was determined before computing the gelation time. Under constant temperature, the time was counted within 1min after the slurry was prepared, and the slurry viscosity was measured regularly at pre-set intervals. Then, the viscosity-time curve of the slurry was plotted. The time corresponding to the viscosity of 100cp was defined as the initial gelation time, while that to the viscosity of 200cp was defined as the final gelation time.

(3) Sweating rate:

The prepared slurry was poured into a 200mL measuring cylinder until reaching 80~90% of the full scale. After standing for 2h, the sweating amount was recorded and divided by the total volume to yield the sweating rate.

(4) Permeability coefficient of the concretion

This coefficient was tested according to the requirements in the Test Code for Hydraulic Concrete (SL352-2006).

(5) Uniaxial compressive strength

The uniaxial compressive strength was tested according to the Method of Testing Cements: Determination of Strength (GB/T17671-1999). The non-vibration moulding was adopted.

The prepared slurry was poured directly into the triple test mould until reaching the upper edge. For each mix proportion, three samples were prepared to perform parallel tests. The mean value was taken as the uniaxial compressive strength of the concretion under the corresponding mix proportion.

The slurries of different mix proportions were prepared to test the initial viscosity of the slurry, the gelation time, the sweating rate, the permeability coefficient of the concretion, and the 28d compressive strength.

2.3. Test results and analysis

The results of the orthogonal test show that the concretion prepared by the mix proportion of A4B1C3D2E2 achieved the smallest permeability coefficient, while that prepared by the mix proportion of A3B4C2D1E4 realized the highest 28d compressive strength.

Therefore, it is recommended to produce reinforced grouting material by the mix proportion of A3B4C2D1E4 ratio configuration (metakaolin: silica sol: silicon powder: quicklime: RLP: composite additive=100:50:25:10:5:10), and to produce anti-seepage grouting material by the mix proportion of A4B1C3D2E2 (metakaolin: silica sol: silicon powder: quicklime: RLP: composite additive=100:60:10:15:3:4).

Considering the limitations of the orthogonal test and the performance features of the raw materials, the above test was further optimized and adjusted, adding several sets of parallel test plans. Finally, the author obtained the following two mix proportions of SPG material for weathered granite grouting, denoted respectively as SPG-I and SPG-II:

(1) SPG-I focuses on reinforcement (mass ratio):

Metakaolin: silica sol: silicon powder: quicklime: RLP: composite additive=100:52:25:9:4:10;

(2) SPG-II focuses on water and seepage prevention (mass ratio):

Metakaolin: silica sol: silicon powder: quicklime: RLP: composite additive= 100:60:9:15:6:5.

The basic performance indices of the two grouting materials are shown in Table 3 below.

3. Mechanical Test on SPG Material

3.1. Uniaxial compressive strength and flexural strength of the concretion and the sand-consolidation body

In actual grouting projects, the slurry is often adopted to consolidate the rock weathering products and fill up rock cracks. Thus, the strength of consolidated rock cannot be evaluated solely based on the strength of the pure slurry concretion. For better evaluation, it is necessary to measure the strength of the sand-consolidation body in each kind of slurry.

The sands for the strength test on sand-consolidation body were collected from the section between Zaoshan Road Station and Licun Station of Qingdao Metro Line 2. The weathering products were excavated from the gaps of the weathered granite, dried naturally, and sieved to leave particles no larger than 2mm. The strength of sand-consolidation body was tested according to the Method of Testing Cements: Determination of Strength (GB/T17671-1999). During the test, the empty test mould and its sleeve were fixed on the swing table, and then the uniformly mixed weathered granite was added into the triple test mould with a spoon until surpassing the mould top by 1~2mm. Next, the stirred slurry was injected slowly into the triple test mould from the upper opening, so that the slurry fully penetrated to all the pores in the weathered granite. After standing for 5min, the mould sleeve was removed and the excess mortar was scraped off from the top of the triple test mould. Then, the mould was relocated to a curing box for curing. The uniaxial compressive strength and flexural strength of the sand-consolidation body were measured on the third, seventh and twenty-eighth days, respectively.

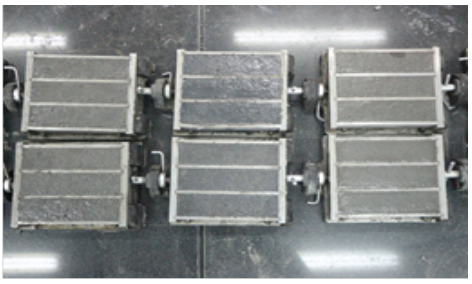

Fig. 1 - Test samples.

The concretion samples were prepared similarly as sand-consolidation body samples, except for the addition of weathered granite.

During the preparation of the concretion sample, the slurry was poured directly into the triple test mould without adding weathered granite. The test samples are presented in Figure 1, and the test results are shown in Table 4 and Figure 2.

Table 3

Basic properties of SPG materials

Type	Initial gelation time (h: min)	Final gelation time (h: min)	Initial viscosity (s)	Sweating rate (%)	Permeability coefficient (10^{-7}cm·s^{-1})	28d compressive strength of the concretion (MPa)
SPG-I	9:26	16:35	26.3	0.8	1.7	14.7
SPG-II	11:43	18:52	25.1	0.6	1.1	9.5

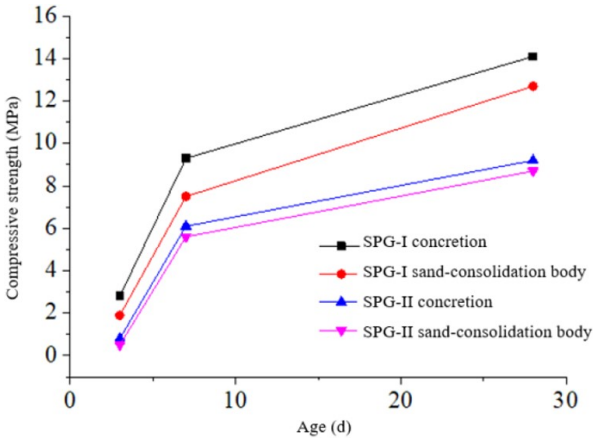

Fig. 2(a) - Compressive strengths of the concretion and solidified sand.

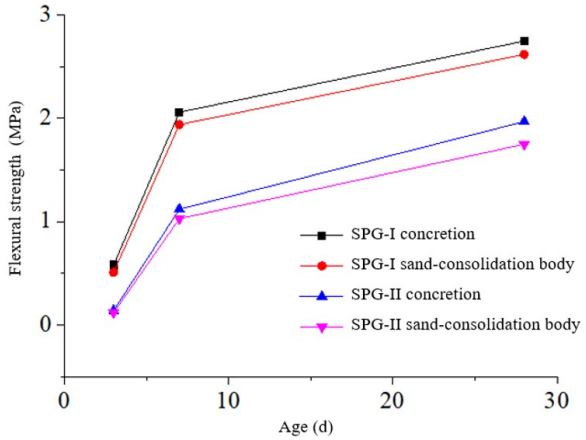

Fig. 2(b) - Flexural strengths of the concretion and solidified sand.

Table 4

Uniaxial compressive strength and flexural strength of the concretion and the sand-consolidation body of SPG materials

Age	SPG-I				SPG-II			
	Compressive strength (MPa)		Flexural strength (MPa)		Compressive strength (MPa)		Flexural strength (MPa)	
	Concretion strength	Sand-consolidation body strength	Concretion strength	Sand-consolidation body strength	Concretion strength	Sand-consolidation body strength	Concretion strength	Sand-consolidation body strength
3d	2.8	1.9	0.58	0.51	0.8	0.5	0.14	0.12
7d	9.3	7.5	2.06	1.94	6.1	5.6	1.12	1.03
28d	14.1	12.7	2.75	2.62	9.2	8.7	1.97	1.75

As shown in Figure 2(a), the uniaxial compressive strength of the concretion of SPG-I was 2.8MPa, 9.3MPa and 14.1MPa, respectively, on the third, seventh and twenty-eighth days, while that of the sand-consolidation body of the same grouting material was 1.9MPa, 7.5 MPa and 12.7MPa, respectively, on the three days. Under the same conditions, the sand-consolidation body was less strong than the concretion. With the elapse of curing time, both materials experienced steady growth in strength.

For SPG-II, the concretion and the sand-consolidation body exhibited a similar strength variation law to that of those of SPG-I, except that the strength was always lower than that of the corresponding material.

It can be seen from Figure 2(b) that the SPG material boasts good flexural strength. The concretion of the SPG-I reached 2.75MPa in flexural strength on the twenty-eighth day and that of the SPG-II reached 1.97MPa on the same day. The 28d flexural strength of the sand-consolidation body of the SPG-I stood at 2.62MPa, while that of the sand-consolidation body of the SPG-2 was measured at 1.75MPa. The high flexural strengths of both concretion and sand-consolidation body are attributable to the uniform distribution of flexible polymer chains in the cured product, which contributes to the resistance of solidified sand.

3.2. Triaxial compression test on the concretion and solidified sand

The triaxial compression test is a relatively mature indoor test method to determine the shear strength of rock under complex stresses. Here, the pseudo triaxial test method is adopted for our research. Cylindrical samples (diameter: 50mm; height: 100mm) were prepared using a self-made plastic mould, and cured for 28d before the test on a TWA-2000 servo rock triaxial test machine. Extensometers were installed in the axial and radial directions of the concretion to measure the axial and radial strains. Before loading, a 0.2kN preload was applied such that the sample was in close contact with the loading device. Then, the confining pressure was increased to the pre-set value at the rate of 15N/s, and maintained constant throughout the test, i.e. the confining pressure should not deviate from the pre-set value by more than 2%. Note that the lateral pressure was kept at a constant value of 1MPa, 3MPa or 5MPa. After that , an axial load was imposed on the sample at an axial displacement rate of 0.2mm/min until the sample was damaged.

The samples were prepared using a ø=5×10cm self-made cylindrical test mould. The water-to-cement ratio was set to 1:1 for the preparation of the concretion samples and sand-consolidation body samples of the SPG materials.

Preparation of concretion samples:

The SPG-I slurry was evenly mixed, and directly poured into the cylindrical test mould. Then, the mould was cured for 24h in a curing box at 25℃ and the relative humidity of 95%. After demoulding, the sample was cured for another 28d before subjected to the triaxial compression test.

The SPG-II slurry was processed through the same steps to prepare concretion samples.

Preparation of sand-consolidation body samples:

The ISO standard sand in China was adopted for the strength test on solidified sand. Firstly, the standard stand was added into the cylindrical test mould, and compacted lightly to make the total mass of the mould and the sand 315g. Then, the SPG-I slurry was slowly poured into the test mould. The slurry filled up the mould due to gravity and slurry permeability. Next, the mould was cured for 24h in a curing box at 25℃ and the relative humidity of 95%. After demoulding, the sample was cured for another 28d before subjected to the triaxial compression test. The SPG-II slurry was processed through the same steps to prepare concretion samples. The test samples are presented in Figure 3, and the test results are shown in Figures 4 and 5.

Fig. 3 - Test samples.

(1)Triaxial compression test results on concretions:

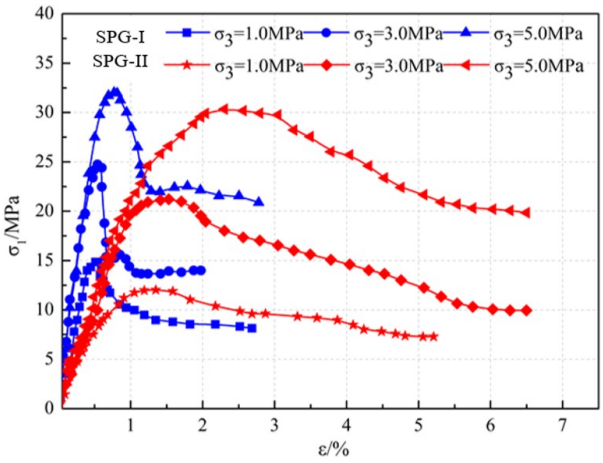

Fig. 4 - Triaxial compression curves of the concretions.

As shown in Figure 4, with the increase in confining pressure, the peak strengths of the concretions of both SPG-I and SPG-II were on the rise and greater than the corresponding unconfined compressive strengths. Comparing the two SPGs, it can be seen that the peak strength of SPG-I was higher than that of SPG-II. The curve of SPG-I was relatively “steep”, revealing a high brittleness. By contrast, the SPG-II was more resilient and better at adapting to deformation than the SPG-I, which is favourable for seepage prevention and water plugging.

(2) Triaxial compression test results on solidified sands

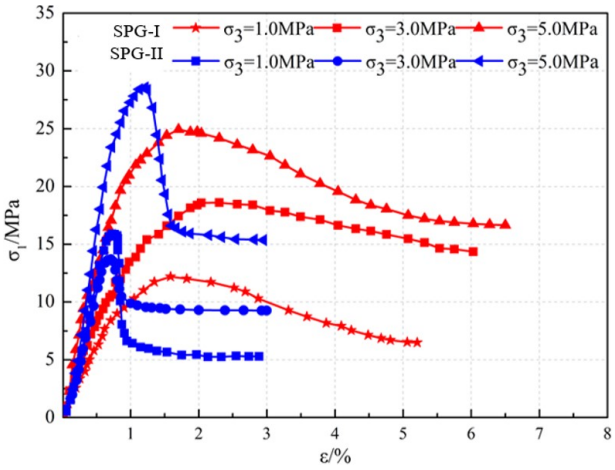

Fig. 5 - Triaxial compression curves of the solidified sands.

It can be seen from Figure 5 that the peak strengths of the solidified sands of both SPG-I and SPG-II were on the rise with the growth in confining pressure. Under the same confining pressure, the sand-consolidation body of SPG-II had a lower peak strength than that of SPG-I, but outperformed the latter in strain capacity.

The triaxial compression curves of the sand-consolidation body were similar to those of the concretions. Under the same conditions, the sand-consolidation body strength was lower than the concretion strength.

Overall, there are many similarities between the triaxial compression curves of the concretions and solidified sands of the two grouting materials and those of ordinary granite, except for the reduced peak strengths and improved strain capacities. The triaxial compression performance of the proposed SPGs can satisfy the application in underground engineering.

(3) Basic mechanical indices of the concretions

The elastic modulus, internal friction angle and internal cohesion of the concretions were derived from the curves in Figures 4 and 5 by the following method.

The elastic modulus E of the rock was approximated from the straight section (the elastic deformation phase) of each curve; the internal friction angle and internal cohesion of the concretions were calculated using the molar stress circle based on the triaxial compression test results under different confining pressures. The resulting basic mechanical indices of the concretions are listed in Table 5 below.

Table 5

Mechanical parameters of the concretions

Type of concretion	Elastic modulus	Internal cohesion	Internal friction angle
SPG-I	4159	3.60	34.7
SPG-II	1178	2.98	53.6

3.3. Bonding strength

In geotechnical engineering, the grouting reinforcement carriers are mainly rock masses and soils with such defects as cracks, fissures and holes. Therefore, the bonding strength to the rock mass and soil is an important indicator of the grouting material. Since the SPG materials only target the anti-seepage reinforcement of weathered granite formation, the bonding strength test only needs to verify the bonding strength of the grouting materials to granite.

The bonding test was conducted according to *the Standard for Test Method of Performance on Building Mortar* (JGJ/T70-2009), only that the base cement mortar was replaced with base granite.

(1) Preparation of base granite samples

Typical granite samples were collected from the construction site of the section between Zaoshan Road Station and Licun Station of Qingdao Metro Line 2, and cut into 70mm×70mm×20mm blocks for further use. The metal moulding frame for the test has an outer frame size of 70mm × 70mm, an inner frame size of 43mm × 43mm, and a thickness of 3mm.

(2) Preparation of tensile bonding strength samples:

The moulding frame was placed on the moulding surface of the base granite specimen. Then, the test slurry was poured into the frame until filling up the frame. After standing for 12h, the sample was taken out from the mould and cured to the required age at 23±2°C and the relative humidity of 60%. After that, the specimen was subjected to the test on tensile bonding strength. The test results are shown in Table 6.

Table 6

Bonding strengths of SPG slurries

Age	SPG-I	SPG-II
14d (MPa)	0.52	0.39
28d (MPa)	0.67	0.45

As shown in Table 1, the tensile bonding strength of the SPG-II to granite was 0.39MPa and 0.45MPa on the fourteenth and twenty-eighth days, respectively; the SPG-I achieved a higher tensile bonding strength to granite: 0.52MPa on the fourteenth day and 0.67MPa on the twenty-eighth day. The results show that the high permeability grouting material has a good bonding strength to granite and can stitch the broken rock into a whole.

4. Engineering Application of SPG Materials

4.1. Project background

The 823m-long section between Zaoshan Road Station and Licun Station of Qingdao Metro Line 2 has a design mileage of YSK47+251~YSK48+074. This is a single-track tunnel with a diameter ofφ=6.1m. The floor and roof are buried respectively at the depth of 24.2~34.1m and 18.2~28.0m. In this section, the distance between the centres of tracks changes gradually from 13.5m in Zaoshan Road Station to 17m in Licun Station.

There are many buildings above this section, as it lies beneath the planned Zaoshan Road. Meanwhile, the section tunnel passes through the Licun River (total length: 14.5km; drainage area: 127.8km2; gradient: 0.713%). At the crossing, the riverbed has been hardened, and the main river channel is 2.0 wide without any anti-seepage treatment. The water, 10.5m in water level elevation and 0.5m in depth, belongs to the category of domestic sewage. Currently, the riverbed serves as a farmer's market.

4.2. Geological disasters

The section tunnel, excavated by the mining method, lies in intensely and even completely weathered granite. The formation is highly stratified and the surrounding rock is very broken. When the tunnel was excavated to ZSK47+956, severe water leakage and rockfall occurred at the face, posing a serious threat to construction and engineering safety. The construction team immediately stopped construction and conducted preliminary shotcreting. After that, a prospect hole was drilled to detect the geological conditions behind the face. Pressurized water jets were discovered when the hole reached the depth of 3m (Figure 6). The drilling was terminated right away to ensure face safety. It is tested that the water flows at 500mL/s from the hole, putting the daily discharge at 43m^3/d. No sediment was found in the water flow. The drilling results show that the surrounding rock becomes soft after 1m behind the face. Currently, the face is located beneath Building No.5 of Shuyuan Road, near Building No.4, Building No.1 and the facade rooms on Jingkou Road. The dense buildings raise strict requirement on ground settlement control of the tunnel.

Fig. 6 - Prospect hole on the face.

4.3. Treatment plan

In light of hydrogeological, monitoring, geological and geophysical data, the full-section curtain grouting was selected for the treatment area. The grouting area reached 3m outside the excavation contour line, the grouting length was 10m, and a 3m retaining wall was built in advance. Forward grouting was conducted after installing the orifice pipe into the holes drilled by the down-the-hole drilling machine.

4.3.1. Construction process

During curtain grouting, the grouting hole was drilled in the face for grout injection. The grout can squeeze out the water in the excavated surface and its surroundings. In this way, the cracks of the surrounding rock were filled up by the grout of certain strength. The grout integrated with the rock mass, forming a water-stopping curtain. The curtain grouting was implemented through the following steps: drilling, burying orifice pipe, installing admission valve and protection valve, water pumping, grouting, hole cleaning, grouting, completion.

4.3.2. Construction method

In order to ensure the effect of curtain grouting, the face was sealed up in advance with a 0.50m-thick C25 concrete layer, which serves as the retaining wall. The lower step was adjusted properly because the upper step was too short to provide enough room for the down-the-hole drilling machine.

The outer holes were drilled and grouted before the inner holes. The grouting area reached 3m outside the excavation contour line.

The upper section was grouted before the lower section. In both the upper and lower sections, the holes in the outer ring were grouted before those in the inner ring. In each ring, the grout was injected every other hole.

4.4. Grouting parameters

Forward grouting was conducted at the pressure of 1.5MPa after installing the orifice pipe into the holes drilled by the down-the-hole drilling machine. The grouting amount was controlled at 1~l.5m^3/s. Before connecting the grouting pipe, the airtightness of the pipe was verified through water pumping. The water also flushed the rock fissures to expand the passage for grouting and enhance the compactness of grout plugging.

The grouting was terminated when the final grouting pressure was less than 1.0MPa and the following to criteria were satisfied.

(1) Single-hole termination criterion: The grouting should continue for over 10min after the grouting pressure gradually increased to the designed final pressure; the single-hole grouting amount was basically the same as the designed grouting amount, and the grouting amount at the termination should be less than 20L/min.

(2) Full-section termination criterion: All grouting holes satisfied the single-hole termination criterion with no grout leakage.

4.5. Selection of grouting materials

Ordinary cement slurry was applied first in this site. After reaching the termination criteria, water flowed out from some parts on the face. To verify the effect of curtain grouting with cement slurry, 10% (4) of all grouting holes were drilled at the key parts of the face. The water flows at the four holes were measured as 100mL/s, 140mL/s, 85mL/s, and 125mL/s, all of which are above 50mL/s.

Since the grouting effect was not satisfactory, a round of blasting excavation was carried out, revealing severe water leakage on the face and the roof. The maximum water flow on the face reached 350mL/s, accompanied with the falling of small rocks. To prevent engineering disasters, the construction was called off immediately, the roof and side walls of the excavated tunnel were re-grouted, and a concrete retaining wall was re-built on the face. Finally, the SPG-II material was selected for the second curtain grouting.

The original plan was basically retained, only that the grouting pressure was lowered to 1MPa. To ensure the grouting effect, the grouting was conducted slowly so that the grout could thoroughly infiltrate into the rock mass.

4.6. Evaluation of treatment effect

4.6.1 Seepage flow variation

Fig. 7 - Full-section grouting of the face.

Table 7

Comparison of the physical and mechanical parameters of the rock and soil mass before and after the grouting

Physical index	Water content (%)	Wet density (g/cm^3)	Compression coefficient (MPa)	Compressive modulus (MPa)	Friction angle (°)	Cohesion (KPa)
Pre-grouting	24.99	1.96	0.33	6.34	23.70	38.42
Post-grouting	9~15	2.25	0.24	7.25	24.20	48.33

As shown in Figure 7, the SPG-II material achieved a remarkable water stopping effect through curtain grouting, leaving no obvious water flow from the face. After grouting, the water flow of each hole was measured. Comparatively speaking, JC1 (28mL/s), JC2 (15mL/s) and JC3 (17mL/s) had a greater water flow than JC4, JC5, JC7 and JC8. The water flow at each of the latter four holes was smaller than 10mL/s. The best grouting effect belongs to JC6, which was basically water-free. The water flow analysis of the eight holes indicate that the SPG-II grouting reduced the maximum single-hole water flow from 500mL/s (43m^3/d) to 28mL/s (2.4m^3/d) (below the 2.4mL/s in waterproof standard), putting the water plugging rate at 94.4%. The water stopping effect is much better than that of cement grouting. Thanks to SPG-II grouting, the tunnel could be excavated with little or no water seepage. The results demonstrate that the SPG-II full-section curtain grouting is an effective anti-seepage measure for intensely and even completely weathered granite formation.

4.6.2. Reinforced strength

During the post-grouting excavation, it is observed that the grout filled up the cracks in an evenly, compacted and well-jointed manner. Unlike sand formation or other formations with loose particles, the intensely and even completely weathered granite formation contains many small kaolin particles, whose permeability coefficient is below the level of 10-4cm/s. This unique feature affects the entry method and functional mechanism of ordinary slurry grouting. Owing to its low wettability and poor permeability, the ordinary slurry enters such a formation mainly through splitting, forming branches of slurry veins. By contrast, the SPG-II boasts a high wettability and strong permeability, especially in weathered granite formation. Under the effect of pentation mechanism, this material can enter the weathered formation at a lower grouting pressure than that of ordinary slurry grouting. Without splitting, the grouting process causes no secondary damage to the weathered formation, and helps to maintain the overall stability of the surrounding rock.

Comparing the pre- and post- grouting situations of the face, it can be seen that the grouting squeezed out some of the water contained in the formation and greatly enhanced the formation strength. Under the same grouting pressure, the SPG-II spread to a much wider area than the preliminarily injected cement slurry. Through the mechanical test on concretions, it is learned that the formation strength and bearing capacity were increased markedly and the physical and mechanical parameters of the rock and soil mass were improved greatly through the SPG-II curtain grouting. Table 7 compares the physical and mechanical parameters of the rock and soil mass before and after the grouting.

5. Conclusions

(1) Considering the features of granite and its weathering products, the author prepared SPG materials using the metakaolin, produced through calcination of kaolin powder, silica sol, silicon powder, quicklime, the RLP and several kinds of surfactants. Through triaxial compression tests, two mix proportions of grouting material were recommended: the ratio of reinforced grouting material (mass ratio) - metakaolin: silica sol: silica fume: quicklime: dispersible polymer powder: composite auxiliaries = 100:52:25:9:4:10; the ratio of impervious grouting material (mass ratio) - metakaolin: silica sol: silica fume: quicklime: dispersible polymer powder: composite auxiliaries = 100:60:9:15:6:5.

(2)The proposed SPG materials were subjected to mechanical test. The test results demonstrate that the SPG slurry has low viscosity and high fluidity, enjoys good wettability, permeability and cohesiveness to weathered granite formation, and requires simple steps and a low grouting pressure in construction. With high strength and good impermeability, the proposed SPG materials can needs of common grouting projects in granite formation.

(3) The SPG-II was applied to the anti-seepage reinforcement of a section in Qingdao Metro, and compared with the effect of cement slurry grouting. Compared with cement slurry, the SPG material achieved a remarkable anti-seepage effect and satisfied the anti-seepage requirements, because it set up a longitudinal anti-seepage system in the intensely weathered granite tunnel due to its strong wettability and water absorptivity.

Acknowledgements

This work is supported by Natural Foundation of Shandong Province, China [Grant No. ZR2017MEE069]. Thank you for the support of Natural Foundation of Shandong Province.

REFERENCES

[1].S.J. Miao, Z.J. Yang and C. Long, Micro-mechanical characteristics and cracks revolution laws of migmatitic granite under different loading conditions, Journal of Jiangsu University (Natural Science Edition), 2012, **33**(4), 469-473.
[2].W. Zhang and H.M. Tang, Experimental study of disintegration mechanism for unsaturated granite residual soil, Rock and Soil Mechanics, 2013, **34**(6), 1668-1674.
[3].S.C. Li, W.J. Zhang and Q.S. Zhang, Research on advantage-fracture grouting mechanism and controlled grouting method in water-rich fault zone, Rock and Soil Mechanics, 2014, **35**(3), 744-752.
[4].C. Zhang, J.S. Yang and Y.P. Xie, Experiment and application for grouting materials for karst under conditions of underground water flow before shield tunneling , Chinese Journal of Rock Mechanics and Engineering, 2018, **37**(9), 2120-2130.
[5].H. Shimada, A. Hamanaka and T. Sasaoka, Behaviour of grouting material used for floor reinforcement in underground mines, International Journal of Mining, Reclamation and Environment, 2014, **28**(2), 133-148.
[6].S.C. Li, X. Zhang and Q.S. Zhang, Research on mechanism of grout diffusion of dynamic grouting and plugging method in water inrush of underground engineering , Chinese Journal of Rock Mechanics and Engineering, 2011, **30**(12), 2377-2396.
[7].C.Q. Dai, Z.H. Zhao, L. Wang and X.Z. Lv, Survey on Rheological Behaviour of Weakly Cemented Soft Rock Considering Water Deterioration, Journal of Advanced Oxidation Technologies, 2018, **21**(2), 317-322.
[8].C.Q. Dai, Y.X. Long and Y.L. Lv, Research on seepage-stress coupling analyses of shallow buried and dug vertical overlapping tunnels, International Journal of Heat and Technology, 2018, **36**(3), 817-824.
[9] D. Zhang, Q. Fang and H. Lou, Grouting techniques for the unfavorable geological conditions of Xiang'an subsea tunnel in China, Journal of Rock Mechanics and Geotechnical Engineering, 2014, **6**(5), 438-446.
[10].J.W. Yun, J.J. Park and Y.S. Kwon, Cement-Based Fracture Grouting Phenomenon of Weathered Granite Soil, Geotechnical Engineering, 2017, **21**(1), 232-242.
[11].K. Masumoto, Y. Sugita and T. Fujita, A clay grouting technique for granitic rock adjacent to clay bulkhead, Physics and Chemistry of the Earth, 2007, **32**, 691-700.
[12].Q.S. Wang, H.Q. Xiao and Z.G. Li, Research on the Technology of Single-pipe Drill Level Retrograde Grouting for Completely Decomposed Granit, Journal of Railway Engineering Society, 2008, (7), 74-78.
[13].D.L. Zhang, F. Sun and P.F. Li, Mechanism of composite grouting in subsea tunnel and its plication, Chinese Journal of Rock Mechanics and Engineering, 2005, **31**(3), 445-452.
[14].J.Q. Yuan, W.Z. Chen, S.W. Huang, Mechanism and synergetic treatment technology of water inrush disaster in completely and strongly weathered granite tunnels , Chinese Journal of Rock Mechanics and Engineering, 2016, **35**(S2), 4164-4171.
[15].K. Wang, S.C. Li and Q.S. Zhang, Research and application of the dynamic grouting technology based on comprehensive analysis of geological information, Journal of Railway Science and Engineering, 2016, **13**(12), 2405-2412.
[16].L.Z. Tang, The application and research of lightweight foam cement in the grouting material, Central South University, 2011.
[17].Z. Wan, L. Zhang and J. Liu, Experimental investigation of anti-seepage performance of improved cement-silicate grouting material, Science Technology and Engineering, 2018, **18**(19), 277-282.
[18].Y. Liu, Y. Chen and G. Li, Research on High Performance Grouting Material and Improving Surrounding Rock Mass Strength, Journal of Mining & Safety Engineering, 2012, **6**, 11-17.

****

MANIFESTĂRI ȘTIINȚIFICE / SCIENTIFIC EVENTS

Optimisation 2019

22 October 2019

https://www.worldcement.com/optimisation/

Optimisation 2019 is **an online conference** for professionals in the cement sector. Since this is a completely virtual conference, you can join us from anywhere in the world, absolutely free.

With a range of speakers from leaders in cement technology, covering topics such as:

- Digitalisation & automation
- Grinding optimisation
- Pyroprocessing optimisation
- Online monitoring & process control
- Alternative fuels
- Controlling emissions
- Logistics & dispatch

****